CHEMICAL ENGINEERING TRANSACTIONS
VOL. 117, 2025
A publication of AIDIC
The Italian Association of Chemical Engineering
Online at www.cetjournal.it
Guest Editors: Fabrizio Bezzo, Flavio Manenti, Gabriele Pannocchia, Almerinda di Benedetto

ISBN 979-12-81206-17-5; **ISSN** 2283-9216
DOI: 10.3303/CET25117144

Photocatalytic Degradation Enhancement of Dye on $Bi_{12}O_{17}Cl_2$ through Er^{3+} and Yb^{3+} Doping

Osemeikhian Ogbeifun*, Shepherd M. Tichapondwa, Evans M. N. Chirwa

Water Utilization and Environmental Engineering Division, Department of Chemical Engineering, University of Pretoria, Pretoria, 0002, South Africa
osemeikhianosi@yahoo.com

Photon upconversion effect employing rare earth lanthanides Ytterbium (Yb^{3+}) and Erbium (Er^{3+}) was harnessed in $Bi_{12}O_{17}Cl_2$ to achieve greater light utilisation targeting the large near-infrared (NIR) region of the solar radiation. In this regard, Er^{3+} and Yb^{3+} were doped into $Bi_{12}O_{17}Cl_2$, and the best doping level was determined by measuring the decolourisation rate of rhodamine B on the materials. The photocatalytic decolourisation of rhodamine B dye on Yb^{3+} and Er^{3+} doped $Bi_{12}O_{17}Cl_2$ materials was assessed under visible light and natural sunlight. The best-performing materials were 0.12%Er- and 0.48%Yb-$Bi_{12}O_{17}Cl_2$, which showed 2.84 and 6.46 folds better than pristine $Bi_{12}O_{17}Cl_2$. As expected, the materials displayed enhanced performance under natural sunlight compared to visible light, the reason being the conversion of a significant portion of NIR (52 % – 55 % of the solar spectrum) into UV and visible light, achieving greater solar light utilisation. The upconversion effect conferred by rare earth intensifies the irradiation strength on the material, which enhances the photocatalytic processes. The degradation mechanism was investigated, revealing the involvement of $O_2^{\bullet-}$ and h^+ in the decolourization of the dye. The study findings underscore the potential of utilising natural sunlight, rich in NIR, to activate $Bi_{12}O_{17}Cl_2$ and propel the photocatalytic degradation of pollutants.

1. Introduction

The transition from fossil fuel to renewable energy is necessary because of global warming and the associated detrimental impacts on the globe. Remediation and pollution control take a significant portion of carbon footprint. For example, removing pollutants from water matrix such as advanced oxidation, filtrations (ultra, micro or nano), reverse osmosis, and other non-traditional techniques, takes significant energy inputs, which in most cases come from fossil energy.

Using renewable energy sources for remediation purposes is desirable to reduce greenhouse gas emissions from burning fossil fuels. Photocatalytic process for removal of organic contaminant can address global warming. Photocatalysis can be based on renewable solar energy if semiconductor material is driven by solar energy spectrum. Materials are available that can utilized the major wavelengths from ultra volet (UV) through visible light (vis) to near infra-red (NIR). The preference for vis photocatalysis stems from the need to reduce energy requirement in generating UV and using solar radiation. Powering a UV process consumes more energy compared to VL driven process. The VL process can be driven by abundant solar light. Furthermore, extending the process to cover NIR will be beneficial since VL (42 % – 43 %) and NIR (52 % – 55 %) make up to 94 % – 98 % of the solar spectrum against UV, which makes up only 3%–5% of the solar spectrum (Hassaan et al., 2023).

The solar radiation spectrum has the following composition of UV, vis and NIR as < 5 %, < 50 % and > 50 %, respectively (Sang et al., 2015, Sheng et al., 2023). This indicates that NIR contributes more than half of the total solar radiation and is a worthwhile effort to utilise the NIR portion of the radiation. Upconversion luminescence converts NIR photons into vis (Hao et al., 2021), making the full utilization of the solar spectrum possible. Upconverting materials amongst other applications have been applied in photocatalysis for degradation of dyes (Zhou et al., 2015).

Paper Received: 6 January 2025; Revised: 1 April 2025; Accepted: 15 May 2025
Please cite this article as: Ogbeifun O., Tichapondwa S.M., Chirwa E.M.N., 2025, Photocatalytic Degradation Enhancement of Dye on Bi12O17Cl2 through Er^{3+} and Yb^{3+} Doping , Chemical Engineering Transactions, 117, 859-864 DOI:10.3303/CET25117144

There are suitable materials that can be activated by VL and in few instances by NIR. Materials that can operate up to the NIR region of the of the spectrum is desirable and implies that such materials can utilize almost the entire wavelengths of abundant renewable solar spectrum. To achieve almost full solar spectrum utilization, semiconductor materials have been doped with lanthanides such as Sm^{3+}, Yb^{3+} and Er^{3+}, to achieve up-conversion (UC) effect. In UC, low-energy infrared is converted to high-energy VL and UV radiation (Marimuthu et al., 2019). When the material is excited in infrared, there is luminesce in the VL and UV regions. The effect means the full use of the spectrum for photocatalyst activation.

$Bi_{12}O_{17}Cl_2$ is an ideal visible light photocatalyst absorbing significantly at the UV region up till 550 nm with its suitable band gap energy for VL irradiation. A stretch into the NIR portion of the spectrum will take advantage of the most significant portion of solar spectrum, the NIR, which makes (NIR) 55 % – 60 % of sunlight (Hao et al., 2021).

This study explores the doping of Yb^{3+} and Er^{3+} in $Bi_{12}O_{17}Cl_2$ material and testing for the photocatalytic activity under NIR. It has been shown that co-doping with Yb^{3+} and Er^{3+} significantly enhances the infrared–to-visible conversion in the host material (Pisarski et al., 2017). In Yb^{3+}/Er^{3+} co-doped material, Yb^{3+} serves as the sensitiser and Er^{3+} as the activator ion (Zhang et al., 2019, Regmi et al., 2017). Yb^{3+} ions absorb at the NIR region (973 nm) with only two states. The energy difference between these two states is almost equal to the energy states of Er^{3+}, making energy shift from Yb^{3+} ions to Er^{3+} ions possible (Marimuthu et al., 2019). Thus, Yb^{3+}–Er^{3+} couple is a very efficient UC system.

2. Materials and method

2.1 Chemical

Bismuth (III) nitrate pentahydrate (Bi $(NO_3)_3{\cdot}5H_2O$), Ytterbium (III) nitrate pentahydrate ($Yb(NO_3)_3{\cdot}5H_2O$), Erbium (III) nitrate pentahydrate ($Er(NO_3)_3{\cdot}5H_2O$) (Sigma Aldrich, South Africa), KCl, KIO_3, ethylene glycol, rhodamine B (Rh B), ethanol (Glassworld Pty, South Africa), deionized water.

2.2 Synthesis and Er^{3+}/Yb^{3+} doping of $Bi_{12}O_{17}Cl_2$

The synthesis and doping of $Bi_{12}O_{17}Cl_2$ with Er^{3+} and Yb^{3+} is illustrated in Figure 1, in which 2 mmol () of $Bi(NO_3)_3{\cdot}5H_2O$ was dissolved in 20 mL of ethylene glycol and 0.33 mmol () of KCl was dissolved separately in 5 mL of ethylene glycol. The two solutions were mixed by means of a magnetic stirrer for 1 h. The resultant mixture was transferred to an autoclave and placed in an oven for hydrothermal treatment at 160 °C for 12 h. The autoclave was allowed to cool down and the product was collected and washed with water and ethanol. The product was dried at 60 °C and then calcined at 400 °C for 1 h to obtain yellow $Bi_{12}O_{17}Cl_2$. For Er^{3+} and Yb^{3+} doped BOC, the preparation step introduced the right amount of $Er(NO_3)_3{\cdot}5H_2O$ and $Yb(NO_3)_3{\cdot}5H_2O$. The following doped levels of Er^{3+} and Yb^{3+} in $Bi_{12}O_{17}Cl_2$ were obtained and the materials are labelled as 0.12%ErBOC, 0.24%ErBOC, 0.47%ErBOC, 1.42%ErBOC, 4.16%ErBOC, 0.48%YbBOC, 1.34%YbBOC, 2.87%YbBOC and 4.3%YbBOC and 5.7%YbBOC.

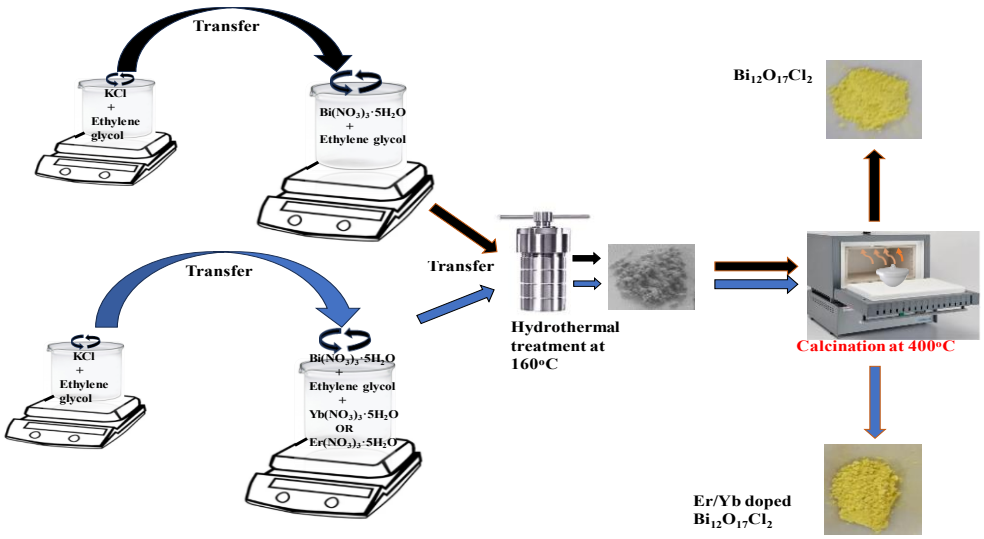

Figure 1: Synthesis and doping $Bi_{12}O_{17}Cl_2$ with Er^{3+} and Yb^{3+}

3. Characterisation of Photocatalyst

3.1 XRD and UV-Vis DRS

XRD and UV-Vis DRS were applied to determine the phase and optical properties of the synthesized materials. Figures 2a and b confirm the successful synthesis of $Bi_{1217}Cl_2$ and doped materials. The XRD pattern of the doped materials showed that the crystalline nature of the material was not lost in the process, as there is consistency in the peak positions. The peak intensity, however, weakened as the doping amounts of Er^{3+} and Yb^{3+} increased. All the peaks of synthesized $Bi_{12}O_{17}Cl_2$ can be assigned to tetragonal $Bi_{12}O_{17}Cl_2$ phase (JCPDS No. 37-0702) which appeared at 2θ = 23.23°, 24.3°, 26.37°, 29.20°, 30.42°, 32.88°, 45.42°, 47.18°, 54.95°, 56.45°, 57.19° and 58.56°, corresponding to (111), (113), (115), (117), (0012), (200), (2012), (220), (307), (315), (317) and (319) crystal planes respectively. (Zhao et al., 2023). For the Er^{3+} and Yb^{3+}-doped $Bi_{12}O_{17}Cl_2$ materials, the peaks were also assigned to the $Bi_{12}O_{17}Cl_2$ phases, indicating that despite doping the material with Er^{3+} and $Yb^{3+,}$ no additional phase(s) were generated. However, a reduction in peak intensity was observed, with increased doping from 0.12%Er/0.48%Yb to 4.16%Er/5.77%Yb. The Bi^{3+} in $Bi_{12}O_{17}Cl_2$ were partly replaced by Er^{3+} and Yb^{3+}, having smaller atomic radii. UV-Vis DRS was performed to investigate the optical properties of the doped material; the result is presented in Figures 2c, and d. As shown, the absorption properties of the material were improved with Er^{3+} and Yb^{3+} doping. The shift in the absorption edge of the material, by doping, altered the band gap energy of doped materials.

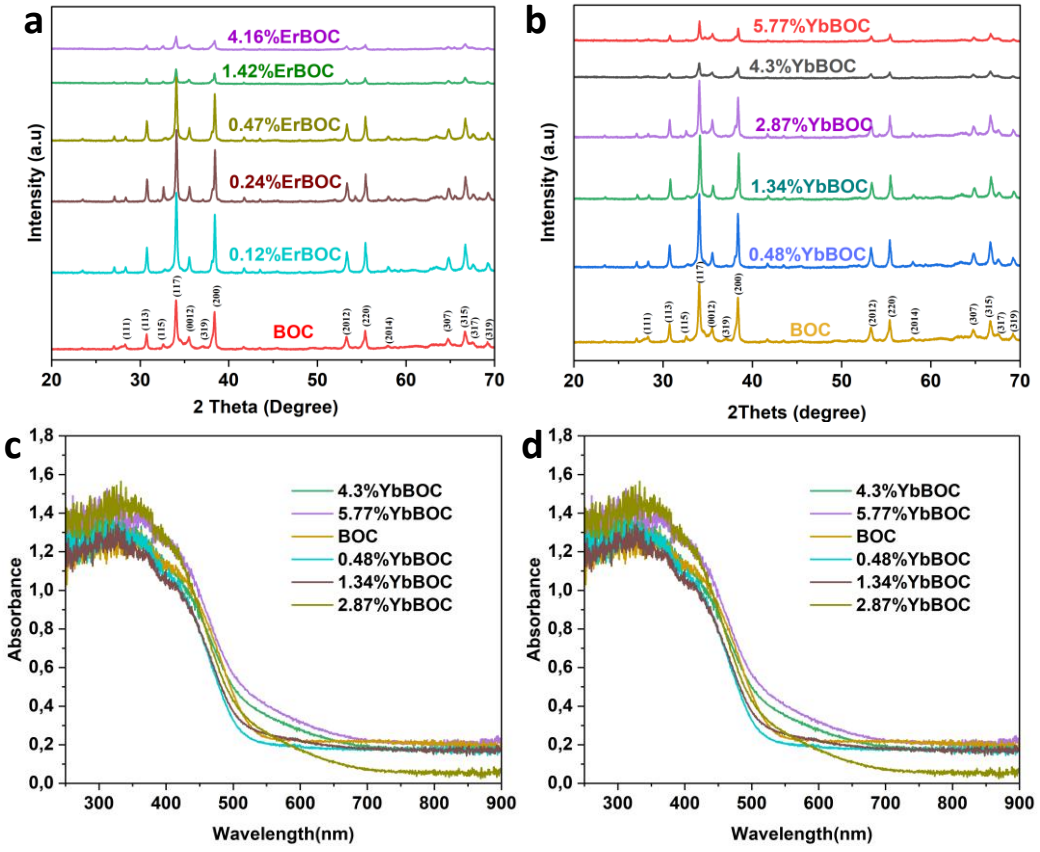

Figure 2: XRD pattern of materials (a), (b), and respective UV Vis DRS spectra (c),(d)

4. Photocatalytic degradation studies

The photocatalytic performances of the material were measured by the rate of decolourisation of rhodamine, which served as the model pollutant. The batch reactor was a 50 mL beaker containing 20 mL of 20 mg/L rhodamine B and dispersed 0.02 g of photocatalyst material. The content was stirred for 1.5 h in the dark to provide absorption desorption equilibrium between the photocatalyst material and the dye. The beaker was irradiated with visible light (λ > 400 nm), and at intervals of 1.5 h, 2 mL aliquot was withdrawn. The absorbance of rhodamine B at 540 nm was used to monitor the concentration of rhodamine B over time.

Figures 3 a and d provide the absorbance peak and concentration of rhodamine B over time. The results in Figure 3 b, c, e and f, showed that the 0.12%ErBOC and 0.48%YbBOC from each category performed best. At 4.5 h hours of light irradiation, the 0.12%ErBOC and 0.48%YbBOC reduced the concentration of rhodamine B from the 20 mg/L initial concentration to 2 mg/L and 0.5 mg/L, respectively. This translates to a degradation efficiency of 80% on 0.12%ErBOC and 95% degradation on 0.48%YbBOC. The degradation results were fitted to the first-order reaction model, -ln(Ct/C0) = t, and the rate constants, k, are shown in Table 1. Important k values are 0.37 h^{-1} for 0.12%Er, 0.80 h^{-1} for 0.48%ErBOC and 0.13 h^{-1} for BOC, which indicate a significant shift in the reaction rate due to Er^{3+} and Yb^{3+} doping. Doping expanded the utilisation of light beyond visible light, generating more charge carriers and leading to improved photocatalytic ability in the doped materials. The UC effect conferred by doping rare earth in the material also leads to broader light utilisation, availing more charged carriers and radicals for degradation.

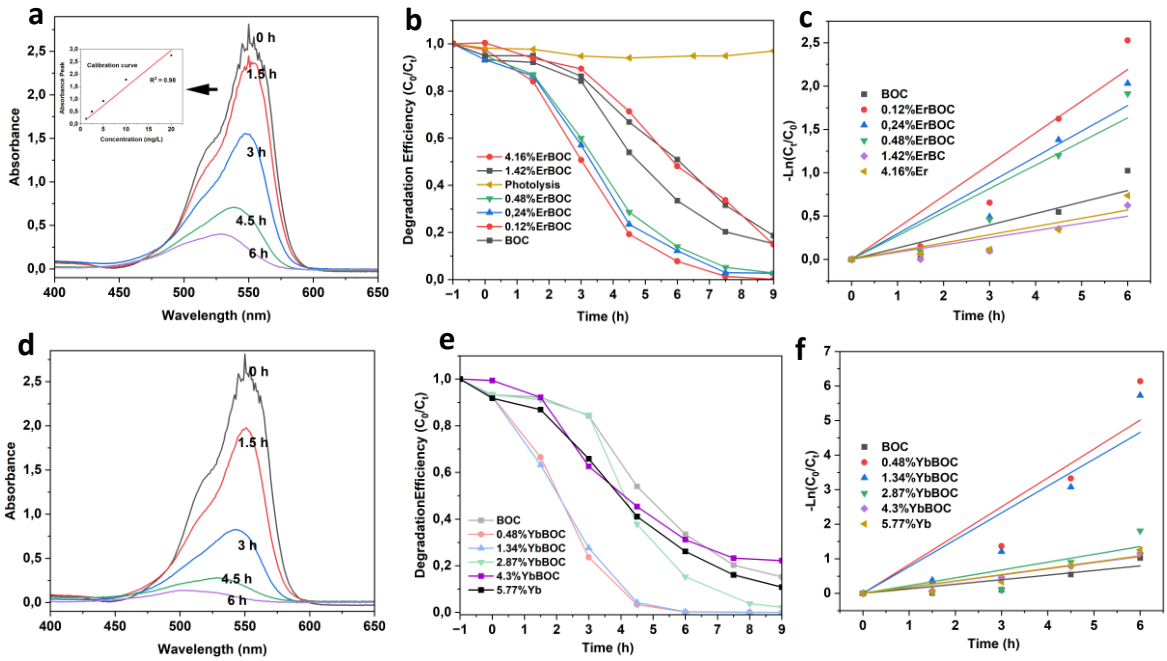

Figure 3: Absorption spectra of rhodamine over 0.12%ErBOC, Inset: calibration curve (a), 0.48%YbBOC (d). Degradation of rhodamine B on x%ErBOC (b), x%YbBOC (c). The pseudo-first-order reaction kinetics of rhodamine B over x%ErBOC (c), and x%YbBOC materials (f)

Table 1: First-order kinetics data

Material	k (h^{-1})	R^2
BOC	0.13	0.87
0.12%ErBOC	0.37	0.95
0.24%ErBOC	0.30	0.94
0.48%ErBOC	0.27	0.94
1.42%ErBOC	0.083	0.89
4.16%ErBOC	0.094	0.90
0.48%YbBOC	0.84	0.93
1.34%YbBOC	0.78	0.93
2.87%YbBOC	0.23	0.84
4.3%YbBOC	0.18	0.98
5.77%YbBOC	0.18	0.95

5. Degradation mechanism

Radical scavenging experiments were conducted to determine the reactive species involved in the photocatalytic process. $AgNO_3$ (e^- scavenger 2 mM; 5.1 mg), Ethylenediaminetetraacetic acid, EDTA-Na (h^+ scavenger 2 mM, 8.8 mg), para-benzoquinone, *p*-BQ($O_2^{\bullet-}$ radical scavenger 1 mM, 1.6 mg), Isopropyl alcohol

(IPA) (·OH radicals scavenger, 5.7 µL 5 mM) (Wang et al., 2022). At the instant of activation of the material by light energy, electrons (e^-) and holes (h^+) are produced. The (e^-) reacts with dissolved oxygen (O_2) in the solution to produce superoxide ($O_2^{\bullet-}$). The h^+ reacts with water (H_2O) to produce hydroxyl radicals. In this instance, the trapping experiment, Figure 4, showed the following percentage decolorization of the dye: No scavenger (100%), $AgNO_3$ (96 %), IPA (85 %), p-QB (40 %), EDTA (4.9 %). The results point to h^+ and $O_2^{\bullet-}$ as the main species in the degradation, while e^- and $OH^\bullet$ played supporting roles.

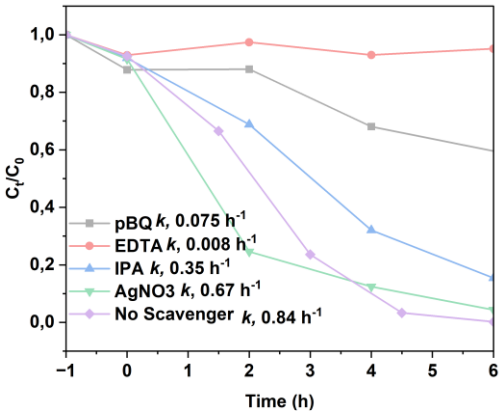

Figure 4: Radical trapping experiment showing the extent of radical involvement in degradation.

The following equation proposes the reaction that occurs in the system.

(1) 0.48%YbBOC + hv → $h^+ + e^-$

(2) $e^- + O_2 \rightarrow O_2^{\bullet-}$

(3) $h^+ + H_2O \rightarrow OH^\bullet + H^+$

(4) $h^+ + OH^- \rightarrow OH^\bullet$

(5) Rhodamine dye + ($OH^\bullet/e^-/OH^\bullet/O_2^{\bullet-}$) → degradation products

6. Conclusions

The photocatalytic strength of $Bi_{12}O_{17}Cl_2$ was improved by doping with rare earth Er^{3+} and Yb^{3+}. The rare earth converts low-energy irradiation in the NIR to visible light. The improved photocatalytic activity of $Bi_{12}O_{17}Cl_2$ by rare earth upconversion effect is significant for solar activation, which has approximately a 45 % NIR, implying a sustainable process that requires less energy. The optimum doping at 0.12%ErBOC and 0.48%YbBOC was determined. Decolourisation/degradation of rhodamine dye on the Er^{3+} - and Yb^{3+} doped $Bi_{12}O_{17}Cl_2$ was 2.84 and 6.46 times faster than on pure $Bi_{12}O_{17}Cl_2$ material. The doped materials are also valuable in removing other organic pollutants from the environment. In addition, the ability of the doped materials to function not only in the visible region of solar radiation but also in NIR implies a reduction in cost in running a photocatalytic system. The target is to rely on natural solar light to activate the photocatalytic degradation of contaminants. The study further highlights using clean energy, i.e. solar, in photocatalytic systems.

References

Hao S., Shang Y., Hou Y., Chen T., Lv W., Hu P., Yang C., 2021. Enhance the performance of dye-sensitized solar cells by constructing upconversion-core/semiconductor-shell structured NaYF4:Yb,Er @BiOCl microprisms. Solar Energy. 224, 563-568. https://doi.org/10.1016/j.solener.2021.05.090

Hassaan M. A., El-Nemr M. A., Elkatory M. R., Ragab S., Niculescu V.-C., El Nemr A., 2023. Principles of Photocatalysts and Their Different Applications: A Review. Topics in Current Chemistry. 381, 31. 10.1007/s41061-023-00444-7

Marimuthu N., Rathnakumari M., Suresh Kumar P., Upadhyay R. B., 2019. Dual photoluminescence emission of Er3+, Yb3+ and Er3+/Yb3+ doped La3Ga5.5Nb0.5O14 ceramics under UV and IR excitation. Journal of Materials Science: Materials in Electronics. 30, 17424-17431. 10.1007/s10854-019-02092-4

Pisarski W. A., Janek J., Pisarska J., Lisiecki R., Ryba-Romanowski W., 2017. Influence of temperature on up-conversion luminescence in Er3+/Yb3+ doubly doped lead-free fluorogermanate glasses for optical sensing. Sensors and Actuators B: Chemical. 253, 85-91. https://doi.org/10.1016/j.snb.2017.06.074

Regmi C., Kshetri Y. K., Ray S. K., Pandey R. P., Lee S. W., 2017. Utilization of visible to NIR light energy by Yb+3, Er+3 and Tm+3 doped BiVO4 for the photocatalytic degradation of methylene blue. Applied Surface Science. 392, 61-70. https://doi.org/10.1016/j.apsusc.2016.09.024

Sang Y., Zhao Z., Zhao M., Hao P., Leng Y., Liu H., 2015. From UV to Near-Infrared, WS2 Nanosheet: A Novel Photocatalyst for Full Solar Light Spectrum Photodegradation. Advanced Materials. 27, 363-369. https://doi.org/10.1002/adma.201403264

Sheng M., Xue J., Wu G., Liu Y., Bi Q., 2023. LuF3: Yb3+/Tm3+@Lu6O5F8: Yb3+/Tm3+@BiOI for efficient degradation of pollutants under NIR light: Synergy of enhanced upconversion emission and efficient FRET. Journal of Environmental Chemical Engineering. 11, 110784. https://doi.org/10.1016/j.jece.2023.110784

Wang Y., Liu C., Hu H., Lu Q., Wang H., Zhao C., Du F., Tang N., 2022. Fabrication of CuFe2O4/Bi12O17Cl2 photocatalyst with intrinsic p-n junction for highly efficient bisphenol A degradation. Journal of Environmental Sciences. https://doi.org/10.1016/j.jes.2022.09.003

Zhang Q., Yang F., Xu Z., Chaker M., Ma D., 2019. Are lanthanide-doped upconversion materials good candidates for photocatalysis? Nanoscale Horizons. 4, 579-591. 10.1039/C8NH00373D

Zhao Y., Liu T., Si W., Cui L., Shi L., 2023. Synthesis and photocatalytic property of a novel Ag2S/Bi12O17Cl2 photocatalyst. Optical Materials. 137, 113557. https://doi.org/10.1016/j.optmat.2023.113557

Zhou J., Liu Q., Feng W., Sun Y., Li F., 2015. Upconversion Luminescent Materials: Advances and Applications. Chemical Reviews. 115, 395-465. 10.1021/cr400478f